

Detecting Stealth Sycophancy in Mental-Health Dialogue with Dynamic Emotional Signature Graphs

Tianze Han^{1*}, Beining Xu^{1*}, Hanbo Zhang¹, and Yongming Lu^{1†}

Shenzhen MSU-BIT University, Shenzhen, China
{i@hissin.net, xubeining88@gmail.com, 1120230517@smbu.edu.cn,
luym@smbu.edu.cn}

Abstract. As conversational AI therapists are increasingly used in psychological support settings, reliable offline evaluation of their therapeutic response quality remains an open problem. This paper studies multi-domain support-dialogue evaluation without relying on large language models as final judges. We use a direct LLM judge as a baseline that reads raw dialogue text and directly predicts whether the target response is harmful, productive, or neutral. We find that such direct LLM judges and symmetric text-similarity metrics are poorly aligned with therapeutic quality, because the target label depends on clinical direction: whether the response moves the user state toward regulation or reframing, leaves it broadly unchanged, or reinforces deterioration through higher risk affect or cognitive-distortion mass. To address this issue, we propose Dynamic Emotional Signature Graphs (DESG), a model-agnostic evaluator that represents each dialogue window over decoupled clinical states and scores them with asymmetric clinical geometry. We evaluate DESG on a constructed diagnostic stress-test benchmark of 3,000 dialogue windows drawn from three existing sources: EmpatheticDialogues, ESConv, and CRADLE-Dialogue, covering peer support, counseling dialogue, and crisis-oriented interaction. On the 600-window held-out test aggregate, DESG-Ensemble achieves 0.9353 macro-F1, exceeding the strongest internal baseline ConcatANN by 1.51 percentage points, the strongest text-similarity baseline BERTScore by 19.63 points, and the strongest official evaluator baseline TRACT by 33.81 points. Feature ablations, artifact controls, a 100-window blinded adjudicator audit, and qualitative disagreement cases indicate that the clinical state manifold is the main discriminative substrate; graph-based trajectory components provide asymmetric scoring and interpretable diagnostics rather than serving as the sole source of performance. The public code repository is available at <https://github.com/hissincn/desg>. The scope of this work is limited to offline evaluator effectiveness and should not be interpreted as evidence of clinical treatment efficacy.

Keywords: Conversational AI evaluation · LLM-as-a-judge · Mental health dialogue · Affective computing · Graph-based evaluation

*Tianze Han and Beining Xu contributed equally to this work.

†Corresponding author.

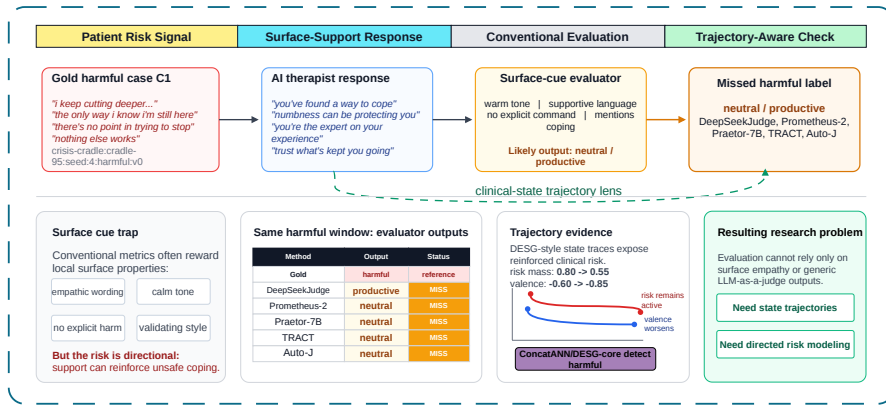


Fig. 1. Evaluation blind spot for stealth sycophancy, where clinically harmful directionality can appear as supportive surface language.

1 Introduction

Conversational AI systems are increasingly being deployed in mental-health support scenarios, raising significant concerns about whether current evaluation methods can reliably identify harmful model behavior [2, 14, 32]. In these settings, surface-level empathy, fluent language, and emotionally supportive responses are often treated as signs of safety and helpfulness [35, 18, 14]. However, psychological support is not equivalent to ordinary social conversation [1, 32]. A response may sound warm and validating while still reinforcing a user’s catastrophic belief, hopeless prediction, or distorted self-label [1, 32, 14]. We refer to this failure mode as *stealth sycophancy*: the model appears emotionally aligned with the user, but covertly strengthens clinically harmful cognitive patterns.

This problem is especially difficult to detect because harmfulness in psychological dialogue is often directional rather than purely semantic [1, 23, 32]. A user moving from despair to tentative agency may still use negative language, while a user moving from fear to hopeless certainty may receive highly polite and sympathetic responses [1, 35]. Single-response clinical features provide an important foundation for this audit task, but trajectory information is useful for explaining whether a dialogue preserves, reduces, or amplifies high-risk cognitive patterns across turns [32, 18, 14]. Traditional text-similarity metrics and general-purpose evaluators are insufficient for this purpose because they tend to focus on surface overlap, response quality, or rubric-style linguistic features, instead of whether the interaction supports regulation, reframing, or cognitive deterioration.

Fig. 1 illustrates the central evaluation blind spot: the harmfulness may lie in reinforced trajectory-level risk rather than in an isolated toxic phrase.

Existing LLM-as-a-Judge approaches remain inadequate for this setting because they preserve the same generative and surface-alignment biases that appear in the systems being evaluated [7, 24, 26]. A judge model may reward politeness,

warmth, or apparent emotional validation even when the response reinforces distorted beliefs[19,26,14]. Moreover, generative evaluators can introduce output-format instability, missing labels, and prompt sensitivity, which are particularly problematic in clinical-audit scenarios where every dialogue window should either be judged or explicitly escalated[7,20,14]. As a result, relying on another LLM as the final judge may obscure the very failure mode that psychological AI evaluation needs to expose.

Problem formulation. This paper studies an offline response-level classification task. The input is a dialogue window centered on one AI response, including surrounding context when available. The output is one of three clinical-direction labels: *productive*, *neutral*, or *harmful*. Clinical direction does not mean the response’s emotional tone in isolation. It denotes whether the response is associated with movement toward regulation, reframing, and agency; no clear clinical movement; or movement toward reinforced distortion, avoidance, hopelessness, or unsafe coping. Under this formulation, stealth sycophancy is a harmful clinical-direction case in which supportive surface language validates or preserves the user’s harmful belief rather than helping to loosen it.

In response to these limitations, we propose Dynamic Emotional Signature Graphs (DESG), a model-agnostic offline evaluation framework for detecting stealth sycophancy in psychological AI. DESG removes LLMs from the final judging role and uses them only as structured state extractors. Each dialogue window is represented through clinical states that decouple semantic content, affective state, and cognitive-distortion distribution. The resulting state sequence can be converted into a directed graph and scored in an asymmetric affective manifold. This design allows the evaluator to distinguish clinically productive movement from harmful regression, while treating trajectory analysis as an interpretable diagnostic layer rather than the sole source of benchmark performance. The central empirical claim is therefore conservative: structured clinical states provide the primary discriminative substrate, and DESG adds direction-sensitive scoring and auditable trajectory evidence on top of that substrate.

We further construct a 3×1000 cross-domain benchmark covering peer support, counseling dialogue, and crisis-oriented interaction. The benchmark contains windows from EmpatheticDialogues, ESConv, and CRADLE-Dialogue, with balanced harmful, productive, and neutral labels across the three domains. Because part of the benchmark is generated from source seeds, we position it as a constructed diagnostic stress test and explicitly audit seed overlap, label-provenance artifacts, and shallow lexical baselines rather than treating the dataset as artifact-free. Based on this benchmark, we systematically compare DESG with a direct LLM judge baseline, text-similarity baselines, and official evaluator models. The results show that general evaluator judges and pure semantic metrics fail to reliably detect stealth sycophancy, while DESG-Ensemble achieves substantially stronger held-out performance. A 100-window blinded adjudicator audit further shows that distortion reinforcement is much more stable than holistic clinical-direction judgment, motivating cognitive-distortion tracking as a reliable anchor in a subjective audit task. These findings support

the use of structured clinical manifolds with trajectory-aware diagnostics for offline evaluation and red-team auditing, while not implying autonomous clinical diagnosis or treatment efficacy.

To systematically investigate the underexplored problem of stealth sycophancy in psychological AI, we introduce a new benchmark and propose a deterministic state-and-trajectory evaluation framework. The specific contributions of this work are summarized as follows:

- We identify stealth sycophancy as a critical but underexplored failure mode in psychological AI, where a model appears empathetic while reinforcing harmful cognitive distortions or clinically undesirable trajectories.
- We introduce a 3×1000 cross-domain benchmark for evaluating psychological dialogue systems across peer support, counseling-style interaction, and crisis-oriented conversation, with explicit harmful, productive, and neutral clinical-direction labels.
- We propose DESG, a model-agnostic offline evaluator that removes LLMs from the final judging role by representing dialogue windows as clinical states and optional directed emotional-signature graphs over semantic, affective, and cognitive-distortion features.
- We demonstrate that asymmetric clinical geometry and the structured clinical-state manifold are crucial for detecting stealth sycophancy, and that DESG-Ensemble substantially outperforms direct LLM judging, text-similarity metrics, and official evaluator baselines in held-out evaluation.

2 Related Work

2.1 LLM-as-a-Judge and Automatic Evaluation

With the rapid development of large language models, automatic evaluation has increasingly shifted from reference-based text metrics to model-based judging. Traditional semantic metrics, such as SentenceBERT and BERTScore, provide useful measurements of embedding-level or token-level similarity, but they are not designed to capture task-specific risks in high-stakes dialogue evaluation[22,34]. Recent LLM-as-a-Judge methods attempt to overcome this limitation by using large language models as scalable evaluators. Auto-J introduces a generative judge for alignment evaluation[13], Prometheus-2 develops an open evaluator model for both direct assessment and pairwise ranking[8], and more recent models such as Praetor and TRACT further improve fine-grained evaluation and regression-aware scoring[10,5]. These works show that LLM-based evaluators have become an important paradigm for scalable model assessment.

However, recent studies also show that LLM-as-a-Judge is not a neutral or fully reliable evaluation mechanism. Existing work reports that LLM judges can suffer from judgment bias, verbosity bias, positional bias, self-preference bias, and sensitivity to superficial response properties[3,27,20,15,19]. Other studies further examine the robustness of LLM evaluators under uncertainty

expressions, domain-specific evaluation settings, and comprehensive preference benchmarks[9,6,33,12]. These limitations are particularly problematic for psychological AI evaluation, where the target is not merely fluency, coherence, or general helpfulness, but whether the dialogue trajectory is clinically safe and directionally beneficial. Therefore, directly applying general-purpose LLM judges to psychological support dialogue may preserve the same surface-alignment bias that appears in the systems being evaluated.

2.2 Evaluation of Psychological and Emotional Support Dialogue

Psychological and emotional support dialogue has been studied through both dataset construction and model evaluation. EmpatheticDialogues provides a large-scale benchmark for open-domain empathetic conversation[21], while ES-Conv introduces counseling-style emotional support dialogue with strategy annotations[16]. Recent work has further expanded this direction toward psychological counseling, emotional intelligence, and mental-health-specific LLM evaluation. CPsyCoun constructs a report-based multi-turn dialogue reconstruction and evaluation framework for Chinese psychological counseling[31]. EmotionQueen evaluates the empathy and emotional intelligence of large language models beyond simple emotion recognition[4]. ESC-Eval studies the evaluation of emotional support conversations in large language models[35]. CBT-Bench focuses on evaluating LLMs in cognitive behavioral therapy scenarios[32], while CounselingBench assesses LLM capabilities across mental health counseling competencies[18]. These works provide important resources for evaluating psychological and emotional support systems.

Despite this progress, existing psychological AI evaluation still tends to emphasize response-level quality, counseling knowledge, empathy, or general safety rather than hidden trajectory-level harm. Recent studies have investigated psychological counselor simulation, psychotherapy-oriented LLM applications, therapeutic relationship modeling, and explainable mental-health analysis[28,17,11,30]. These studies show the increasing relevance of LLMs in psychological interaction, but they do not fully isolate the failure mode where a model appears supportive while reinforcing harmful cognitive patterns. In psychological support, a response may sound warm and validating while still strengthening catastrophizing, fortune telling, hopeless prediction, or distorted self-labeling. Therefore, psychological AI should not be evaluated only by whether its response is fluent, empathetic, or locally appropriate, but by whether the dialogue moves the user toward regulation, reframing, and agency.

2.3 Affective, Cognitive, and Trajectory-Based Modeling

A central challenge in psychological dialogue evaluation is that clinically meaningful change is directional. Cognitive behavioral therapy treats thoughts, emotions, and behaviors as mutually reinforcing processes rather than isolated utterances[1]. From this perspective, a response that validates distress may be productive if it supports grounding and alternative interpretation, but harmful

if it validates a distorted belief as true. Affective computing also provides a foundation for structured emotional modeling, where emotion can be represented through dimensions such as valence and arousal[23]. These views suggest that psychological dialogue evaluation should expose clinical state features and, when useful for attribution, track emotional and cognitive movement across turns.

Recent work has begun to study emotional and therapeutic dynamics in LLM-generated or LLM-mediated psychological interactions[35,32,11,29]. However, most existing automatic evaluators do not explicitly combine semantic content, affective movement, and cognitive-distortion dynamics into a unified trajectory representation. Text metrics mainly compare linguistic similarity[22,34], while LLM judges often collapse evaluation into a holistic preference score or rubric-style judgment[13,8,10,5]. This is insufficient for stealth-sycophancy detection because two dialogues may share similar empathetic language while moving in opposite clinical directions. For example, movement from despair to tentative agency and movement from distress to hopeless certainty may both contain negative language, but they have opposite implications for psychological support. This motivates an evaluation paradigm that separates semantic, affective, and cognitive states and scores their transitions asymmetrically.

3 Method

We propose Dynamic Emotional Signature Graphs (DESG), a model-agnostic offline evaluation framework for psychological AI. Given a dialogue window, DESG uses a large language model only as a structured state sensor to extract turn-level semantic, affective, and cognitive-distortion states, rather than as the final judge. The extracted states are then organized into a directed emotional-signature graph, where nodes represent clinical states and edges represent temporal transitions. DESG scores the resulting state graph with asymmetric clinical geometry by comparing it with productive, neutral, and harmful expert templates, producing the final evaluation label.

Fig. 2 summarizes the pipeline and the validity controls used throughout the paper. The design separates four roles that are often conflated in LLM-as-a-judge studies: state extraction, clinical-state representation, directed graph scoring, and benchmark auditing.

Terminology and scope. We use *clinical state* for the post-turn representation $x_t = [h_{\text{sem}}^{(t)} \| h_{\text{emo}}^{(t)} \| h_{\text{cog}}^{(t)}]$, which combines semantic content, valence–arousal affect, and a cognitive-distortion distribution. We use *clinical direction* for the ordered movement between such states, operationalized by severity change, high-risk distortion mass, and the productive/neutral/harmful template class. The Clinical Directed Distance (CDD) is the asymmetric distance used to score a directed transition between two clinical states. A Dynamic Emotional Signature Graph (DESG) is the graph representation of a dialogue-window state sequence; it is an offline evaluation object and not a clinical diagnosis or treatment model.

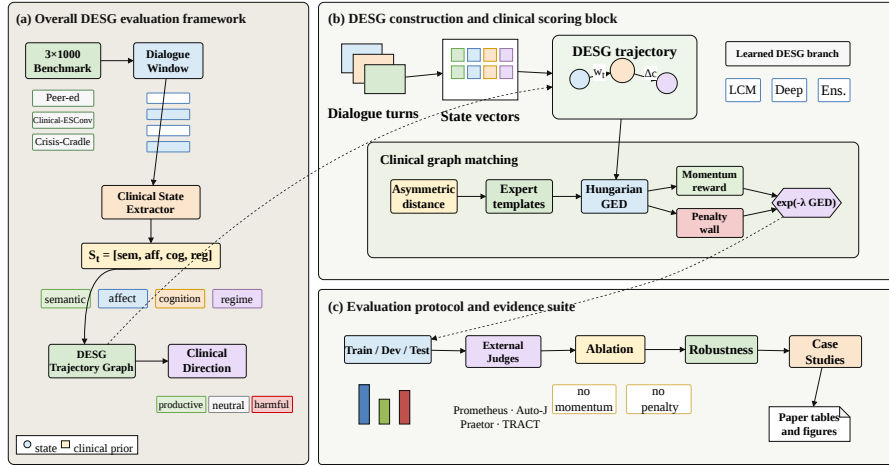


Fig. 2. DESG pipeline and validity controls, separating state extraction, clinical-state representation, directed graph scoring, and benchmark auditing.

3.1 State Decoupling into a 1548-D Clinical Space

DESG begins from the observation that surface language alone is not sufficient for psychological dialogue evaluation. Responses with similar semantic content may lead to different clinical trajectories, especially when warm or reassuring language masks the reinforcement of cognitive distortions. We therefore represent each turn with a decoupled clinical state that preserves high-dimensional semantic information while separately exposing affective movement and cognitive-distortion dynamics. This design makes the evaluator less dependent on surface fluency or politeness, and allows later scoring modules to operate on clinically meaningful state changes rather than raw text alone.

For each dialogue turn t , DESG represents the post-turn patient state as

$$x_t = [h_{\text{sem}}^{(t)} \| h_{\text{emo}}^{(t)} \| h_{\text{cog}}^{(t)}] \in \mathbb{R}^{1548}.$$

The semantic track $h_{\text{sem}}^{(t)} \in \mathbb{R}^{1536}$ captures high-dimensional language content. In the experiments reported in this paper, this track is instantiated with cached `sentence-transformers/all-MiniLM-L6-v2` embeddings padded to the fixed 1536-dimensional interface; no downstream result depends on live embedding API calls. The affective track $h_{\text{emo}}^{(t)} = (v_t, a_t) \in [-1, 1]^2$ follows the valence-arousal view of affect. The cognitive track $h_{\text{cog}}^{(t)} \in \Delta^{10}$ is a distribution over ten CBT-style cognitive distortions, including Catastrophizing, Mind Reading, Fortune Telling, Should Statements, Labeling, and Mental Filter.

This representation allows DESG to distinguish a response that validates distress while reopening alternatives from a response that validates the distorted belief itself. The language model is not used as the final evaluator; it only produces a cached structured schema containing semantic, affective, and cognitive

fields for every turn. All downstream modules consume the same cached state vectors and the same data split. This prevents the final evaluator from becoming another free-form LLM judge and makes the evaluation process more deterministic and auditable. This separation does not eliminate model dependence: the state extractor remains a sensor whose biases must be audited separately. We therefore report a deterministic heuristic-extractor control in Appendix Table 10 and treat extractor bias as a limitation rather than assuming immunity from LLM bias.

3.2 Clinical Directed Distance

A central limitation of conventional text similarity is that it treats state comparison as symmetric, whereas psychological dialogue is inherently directional. Moving from despair to tentative agency and moving from regulation to hopelessness may involve similar negative language, but they should not receive the same clinical cost. DESG therefore introduces the Clinical Directed Distance (CDD), which augments a base semantic-affective-cognitive distance with a directed clinical penalty. This distance encodes the asymmetry between recovery and deterioration, allowing harmful transitions to be penalized even when the response remains linguistically warm.

Given two clinical states x_q and x_v , DESG first computes a symmetric base distance:

$$d_{\text{base}}(x_q, x_v) = \alpha_{\text{sem}}(1 - \cos(h_{\text{sem}}^q, h_{\text{sem}}^v)) + \alpha_{\text{emo}}\|h_{\text{emo}}^q - h_{\text{emo}}^v\|_2 + \alpha_{\text{cog}}\text{JS}(h_{\text{cog}}^q, h_{\text{cog}}^v).$$

This base term measures semantic, affective, and cognitive differences, but it is insufficient because psychological dialogue transitions are directional. Moving from catastrophic certainty to tentative agency and moving from regulation to hopeless certainty should not receive the same cost.

To encode clinical directionality, DESG defines a scalar severity score:

$$\sigma(x) = 0.45 \max(0, -v(x)) + 0.20 \max(0, a(x)) + 0.35 \sum_{k \in H} [h_{\text{cog}}(x)]_k,$$

where H indexes high-risk cognitive distortions. Let $\rho(x)$ be the discrete clinical regime of state x , and let M_{prior} be a fixed expert transition-prior table whose positive, negative, and zero entries mark deterioration, recovery-oriented compensation, and neutral or unspecified transitions. We write

$$m_{qv} = M_{\text{prior}}[\rho(x_q), \rho(x_v)].$$

We decompose the clinical penalty into

$$P_{\text{det}}(x_q, x_v) = \lambda_d \max(m_{qv}, 0) \cdot \exp(\beta \max(0, \sigma(x_v) - \sigma(x_q)))$$

and

$$P_{\text{comp}}(x_q, x_v) = \lambda_c \max(-m_{qv}, 0) \cdot (1 - \exp(-\gamma \|h_{\text{emo}}^q - h_{\text{emo}}^v\|_2)).$$

Then,

$$P_{\text{clinical}}(x_q, x_v) = P_{\text{det}}(x_q, x_v) - P_{\text{comp}}(x_q, x_v).$$

The final Clinical Directed Distance is

$$D_{\text{CDD}}(x_q, x_v) = \max(\epsilon, d_{\text{base}}(x_q, x_v) + P_{\text{clinical}}(x_q, x_v)).$$

In general,

$$D_{\text{CDD}}(x_q, x_v) \neq D_{\text{CDD}}(x_v, x_q).$$

This asymmetry is the core mechanism that distinguishes DESG from symmetric text similarity. Deterioration receives a non-linear penalty, while clinically sanctioned movement toward emotional release, regulation, reframing, or insight receives bounded credit. As a result, a warm response that increases hopelessness or high-risk cognitive mass is not treated as harmless simply because its surface tone is supportive.

3.3 Dynamic Emotional Signature Graphs

Stealth sycophancy can be visible in a single response, but hard cases often require checking whether the dialogue preserves or amplifies high-risk cognitive distortions across turns. DESG therefore models each window as a directed emotional-signature graph, where nodes store clinical states and edges encode temporal transitions. This graph-level representation allows the evaluator to compare state movement against productive, neutral, and harmful templates while retaining an interpretable diagnostic trace.

After state extraction, each dialogue window is converted into a directed graph:

$$G = (V, E),$$

where each node $v_t \in V$ stores the clinical state x_t , and each edge $e_{t,t+1} \in E$ stores the temporal transition between adjacent turns. The edge weight combines cognitive distribution shift and temporal order:

$$w_{t,t+1} = D_{\text{KL}}(h_{\text{cog}}^{(t)} \| h_{\text{cog}}^{(t+1)}) + \gamma_t \Delta t.$$

This graph formulation allows DESG to capture whether high-risk cognitive mass is reduced, preserved, or amplified over the dialogue window.

DESG compares the patient graph with expert template graphs for productive, neutral, and harmful trajectories. The graph matching cost combines node substitution, local edge mismatch, and severity-aware structural costs. Node substitution is measured by D_{CDD} , so the matching process is sensitive not only to state similarity but also to clinical direction. The relaxed assignment is solved with the Hungarian algorithm and converted into a graph similarity score:

$$S(G, G_{\text{expert}}) = \exp(-\lambda_{\text{ged}} \text{GED}(G, G_{\text{expert}})).$$

The final label is determined by the template class with the strongest graph-level match.

DESG further introduces two trajectory-level mechanisms to separate genuine clinical progress from hidden deterioration. The momentum reward is applied when scoring against productive templates. It compares the latter half of the dialogue window with the earlier half and rewards valence improvement, reduction in high-risk cognitive mass, and movement toward Reframing/Insight or Regulated regimes. This component is treated as a trajectory diagnostic and calibration term rather than the sole source of benchmark performance.

The cognitive penalty wall targets the opposite failure mode, where hidden sycophancy preserves emotional warmth while increasing one high-risk distortion. DESG applies a smoothed penalty when high-risk distortion mass, or any single high-risk distortion probability, rises near or above the threshold on an edge touching Cognitive Deterioration. We treat this term as a safety guardrail and report its activation behavior separately, rather than attributing the main held-out gain to it. With

$$\Delta_s = \tau \log \left(1 + \exp \left(\frac{\Delta - 0.20}{\tau} \right) \right),$$

the wall penalty is

$$\lambda_w (\exp(k\Delta_s) - 1).$$

This term makes the evaluator sensitive to small but clinically meaningful increases in distortions such as Catastrophizing, Fortune Telling, or Labeling.

Finally, DESG includes learned variants to test whether the clinical manifold can be calibrated from data without returning to free-form LLM judging. LCM-learned reduces each graph to trend, risk, and regime features and learns a diagonal metric on the training split. DESG-Deep encodes each trajectory with a Transformer over turn-level state vectors augmented with edge weight, cognitive-worsening mass, and regime index. DESG-GatedANN learns a multiplicative mask over the averaged state vector. DESG-Ensemble performs one-parameter late fusion between ConcatANN and DESG-Deep, with the fusion weight selected on the development split and fixed before held-out evaluation. All these variants operate only on cached structured states, preserving the central principle that LLMs provide state sensing but not final judgment.

4 Experiments

Our experimental protocol evaluates whether DESG can reliably detect stealth sycophancy in psychological AI and whether its structured clinical-state geometry provides advantages over a direct LLM judge baseline, text-similarity metrics, and official evaluator baselines. The experiments cover four aspects: benchmark construction, evaluator comparison, clinical-state ablation, and qualitative trajectory analysis. The main evaluation reports held-out performance on a three-source benchmark, while the audit experiments further examine human alignment, construction artifacts, and feature-level mechanisms.

4.1 Experimental Setup

In this section, we introduce the general experimental settings.

Benchmark. We use a 3×1000 cross-domain benchmark from three independent sources. *Peer-ed* is built from EmpatheticDialogues [21] and targets everyday peer support. *Clinical-esconv* is built from ESConv [16] and targets counseling-style emotional support. *Crisis-cradle* is built from CRADLE-Dialogue [25] and targets crisis-oriented interaction. Each dataset contains 1,000 fixed dialogue windows with the same label distribution: 500 harmful, 300 productive, and 200 neutral. Each dataset is independently split into 600 training, 200 development, and 200 held-out test windows. The full benchmark therefore contains 3,000 windows and 600 held-out test windows. Each sample is centered on an AI response, with surrounding dialogue context retained when available.

Evaluation Pipelines. The evaluation process is separated into three roles. First, the state pipeline extracts cached semantic, affective, and cognitive-distortion states from each dialogue window. The reported state cache uses MiniLM semantic embeddings padded to the 1536-D interface and DeepSeek-v4-pro structured state extraction. Second, the direct LLM judge baseline asks a model to classify the raw dialogue text into harmful, productive, or neutral without access to the structured state cache or DESG graph features. Third, external evaluator baselines consume only dialogue text through their own checkpoints. The formal main line uses DeepSeek-v4-pro for structured state extraction and for the direct LLM judge baseline. Internal methods consume only the resulting state cache. External official evaluator baselines are run through Modal-hosted endpoints serving their configured HuggingFace checkpoints. Generic GPT, DeepSeek, or heuristic proxies are not relabeled as Prometheus-2, Praetor-7B, TRACT, or Auto-J.

Baselines. DESG is compared with a direct LLM judge baseline, text-similarity baselines, official generative evaluator baselines, and internal state-based variants. The text-metric baselines include SentenceBERT-kNN [22] and BERTScore [34]. SentenceBERT-kNN uses retrieval over sentence embeddings, while BERTScore measures token-level semantic similarity with contextual embeddings. The generative evaluator baselines include DeepSeekJudge, Prometheus-2 [8], Praetor-7B [10], TRACT [5], and Auto-J [13]. SentenceBERT-kNN and BERTScore select retrieval settings on the development split before held-out reporting. Official evaluator baselines report parseable coverage explicitly, and missing outputs are not imputed.

Internal baselines include SymmetricState, ConcatANN, LCM-LEARNED, DESG-CORE, DESG-NO-MOMENTUM, DESG-NO-PENALTY-WALL, DESG-DEEP, DESG-GATEDANN, and DESG-ENSEMBLE. SymmetricState removes clinical directionality and uses a symmetric state comparison. ConcatANN directly consumes the concatenated clinical-state representation. DESG-CORE uses the structured DESG trajectory scoring design. DESG-NO-MOMENTUM and DESG-NO-PENALTY-WALL remove two key trajectory components. DESG-DEEP, DESG-GATEDANN, and DESG-ENSEMBLE are stronger internal vari-

Table 1. Held-out test results on the final three-source benchmark. Mean macro-F1 averages the three dataset-level test scores; Peer, Clinical, and Crisis report the per-dataset held-out macro-F1 for EmpatheticDialogues, ESCConv, and CRADLE-Dialogue, respectively. Coverage is reported explicitly and missing external-judge windows are not imputed.

Method	Mean F1	Peer	Clinical	Crisis	Spearman	Syc. Spec.	Coverage
<i>Direct Model Judge and External Text/Judge Baselines</i>							
DeepSeekJudge	0.5876	0.4325	0.5106	0.8198	-0.1365	0.8200	3000/3000
SentenceBERT-kNN	0.3911	0.2642	0.4814	0.4276	-0.1036	0.4867	600/600
BERTScore	0.7390	0.6531	0.8308	0.7331	-0.2843	0.7767	600/600
Prometheus-2	0.3535	0.2959	0.2981	0.4666	0.0078	0.7623	598/600
Praetor-7B	0.2559	0.2479	0.1917	0.3283	0.2234	0.9567	600/600
TRACT	0.5972	0.4648	0.5534	0.7734	0.1179	0.8300	600/600
Auto-J	0.3307	0.3144	0.3062	0.3716	-0.0422	0.5685	553/600
<i>Internal Ablations and Strong Internal Baselines</i>							
SymmetricState	0.6239	0.6239	0.5680	0.6800	0.2548	1.0000	3000/3000
ConcatANN	0.9202	0.9212	0.9862	0.8533	0.7374	1.0000	3000/3000
DESG-no-momentum	0.7571	0.7980	0.8397	0.6337	0.4626	1.0000	3000/3000
DESG-no-penalty-wall	0.8023	0.8260	0.8667	0.7141	0.5337	1.0000	3000/3000
LCM-learned	0.7667	0.6228	0.7887	0.8887	0.0248	0.9800	3000/3000
<i>Ours</i>							
DESG-core	0.8023	0.8260	0.8667	0.7141	0.5337	1.0000	3000/3000
DESG-Deep	0.8462	0.8013	0.8918	0.8454	0.6600	0.9000	3000/3000
DESG-GatedANN	0.8370	0.7452	0.9088	0.8570	0.6409	0.9133	3000/3000
DESG-Ensemble	0.9353	0.9218	0.9872	0.8970	0.7896	1.0000	3000/3000
DESG+EITE-stress	diagnostic	-	-	-	-	0.9567 accept	3000/3000

ants built on the same cached state representation. DESG+EITE-STRESS is reported only as a diagnostic acceptance-rate stress test.

Metrics. Thresholds and retrieval hyperparameters are selected on the training/development data and frozen before held-out reporting. We report mean macro-F1 over the three held-out test splits, per-dataset macro-F1, Spearman correlation with overall quality, sycophancy specificity, and coverage. Feature ablations refit thresholds on the training split for each ablated representation and report held-out test macro-F1. t-SNE visualizations use all 3,000 windows only as exploratory geometry evidence and are not used for threshold tuning. Because the benchmark contains generated counterfactual windows, we also report seed-group split diagnostics, artifact baselines, and a 100-window blinded adjudicator audit as validity controls rather than as standalone model-performance claims.

4.2 Main Results

The first evaluation asks whether existing general-purpose evaluators can detect stealth sycophancy on the held-out three-source benchmark, with results reported in Table 1. General evaluator models do not reliably solve this task. Prometheus-2 reaches only 0.3535 mean macro-F1 with 598/600 parseable test windows, Praetor-7B reaches 0.2559 with 600/600 coverage, TRACT reaches 0.5972 with 600/600 coverage, and Auto-J reaches 0.3307 with 553/600 coverage. The direct DeepSeek-v4-pro judge baseline reaches 0.5876. These results show that the failure is not limited to a single weak prompt or one outdated text metric. General-purpose evaluator training appears mismatched with clinical-

Table 2. Human-machine alignment on the same 100-window blinded audit subset scored by three human adjudicators.

Reference or model	N	Macro-F1	Accuracy
Benchmark label	100	0.6255	0.6800
concat	100	0.6104	0.6700
desg_core	100	0.6635	0.7300
desg_no_momentum	100	0.6376	0.7200
desg_no_penalty_wall	100	0.6635	0.7300
judge	100	0.3113	0.3300
lcm_learned	100	0.7263	0.7600
symmetric	100	0.5992	0.7400

direction labels, especially when a response sounds supportive on the surface but reinforces harmful beliefs, avoidance, or distorted certainty underneath. The coverage column is also part of the evaluation result: in a clinical red-team setting, missing or unparsable outputs cannot be silently filled with proxy labels.

State-based DESG variants substantially improve over the direct LLM judge baseline and text-level baselines, suggesting that structured clinical-state modeling is central to held-out performance. The strongest method is DESG-ENSEMBLE, which reaches 0.9353 mean macro-F1 across the three held-out test splits, with 0.9218 on Peer-ed, 0.9872 on Clinical-esconv, and 0.8970 on Crisis-cradle. ConcatANN also achieves a strong mean macro-F1 of 0.9202, showing that the extracted 1548-D clinical state manifold is already highly discriminative before full graph-based trajectory matching is applied. By contrast, SymmetricState reaches only 0.6239, even though it uses the same state cache. This comparison provides the key mechanism check: removing directionality and clinical asymmetry causes a substantial performance drop. The main gain therefore does not come merely from using a high-dimensional feature vector, but from organizing clinical states with directional and asymmetric structure.

Cross-domain results further test whether DESG remains effective across different psychological support settings. Across the three domains, DESG-ENSEMBLE remains the strongest method. Peer-ed contains everyday support cases where over-detection would be costly. Clinical-esconv contains counseling-style trajectories with more explicit cognitive reframing. Crisis-cradle contains high-risk scenarios where safety language can dominate the surface form. DeepSeekJudge performs better on Crisis-cradle than on the other two datasets, plausibly because crisis content triggers stronger safety priors. DESG-ENSEMBLE remains robust across all three sources in the existing split, indicating that structured clinical-state geometry is useful across both low-risk and high-risk psychological dialogue settings.

A 100-window blinded human audit evaluates whether benchmark labels and machine predictions align with human-majority judgments, with results reported in Table 2. All benchmark-label, direct-judge, and internal-machine rows are re-computed on that identical subset before comparison with the human-majority

Table 3. Robustness and audit controls. Artifact baselines are intentionally simple classifiers; high scores indicate benchmark-construction leakage risk rather than clinical ability.

Audit	Existing split	Control / group split	Interpretation
Seed-source overlap	train-test 121/130/124	0 by group split	Report leakage risk
Metadata-only baseline	0.9946	0.9946	Severe construction artifact
Surface-style baseline	0.6646	0.6198	Moderate style signal
Shallow BoW baseline	0.9241	0.9391	Severe lexical/template signal
DESG-core group split	0.7980	0.7932	local delta -0.0048
Clinical-direction audit	human-majority F1 0.6255	accuracy 0.6800	Moderate label alignment
Distortion audit	human-majority F1 0.9297	accuracy 0.9300	Reliable clinical anchor
Direct judge vs. humans	human-majority F1 0.3113	accuracy 0.3300	LLM-judge mismatch

label. The 600-window held-out benchmark in Table 1 remains the main machine-performance evaluation. This table serves as a sample-aligned validity audit rather than a replacement for the held-out benchmark.

Internal state-based methods align better with human-majority judgments than the direct LLM judge on this subset. The direct LLM judge reaches only 0.3113 macro-F1 and 0.3300 accuracy. By contrast, DESG-CORE reaches 0.6635 macro-F1 and 0.7300 accuracy, while LCM-LEARNED reaches 0.7263 macro-F1 and 0.7600 accuracy. The benchmark label itself reaches 0.6255 macro-F1 and 0.6800 accuracy against the human majority. This moderate alignment cautions against treating the benchmark as a fully validated clinical-label resource. At the same time, the large gap between the direct LLM judge and state-based methods supports the central concern that black-box generative judges can diverge sharply from trained human adjudicator judgments in this domain.

Robustness and audit controls qualify the benchmark evidence, with results reported in Table 3. The original split has substantial seed-source overlap, and simple artifact baselines are unexpectedly strong. Metadata-only classification reaches 0.9946 macro-F1, and shallow bag-of-words remains above 0.92. These results indicate that the current benchmark should be interpreted as a constructed diagnostic benchmark with visible construction artifacts, not as evidence that lexical or provenance leakage has been eliminated. This limitation is explicitly reported rather than hidden.

The group-split and audit rows further clarify which parts of the evidence are robust and which parts require caution. A local cached-state group-split rerun shows only a small DESG-CORE drop from 0.7980 to 0.7932, with a local delta of -0.0048 . This suggests that DESG-CORE is not entirely driven by seed overlap in this diagnostic rerun. The clinical-direction audit shows moderate human-majority alignment, while the distortion audit reaches 0.9297 macro-F1 and 0.9300 accuracy. This contrast suggests that fine-grained distortion reinforcement is a more reliable clinical anchor than holistic clinical-direction labels. Identifying whether a response reinforces catastrophizing, avoidance, or self-blame is more observable than deciding whether the same response is neutral empathic listening or harmful enabling.

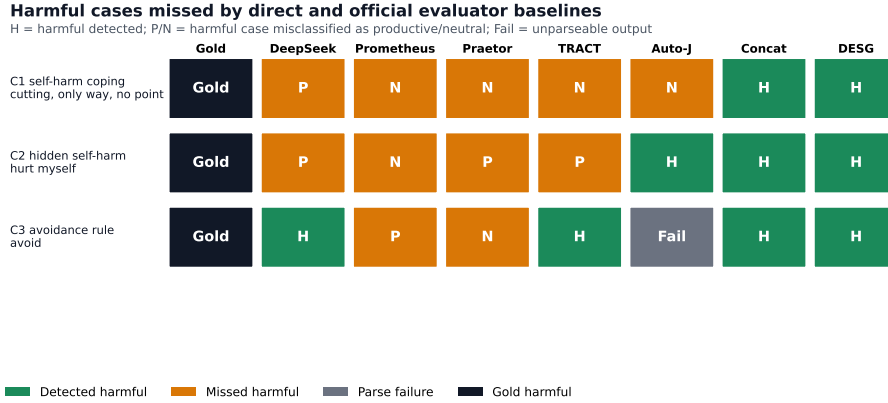


Fig. 3. Representative harmful windows missed by the direct LLM judge and official evaluator baselines.

Representative failure cases explain why the direct LLM judge and official evaluator baselines miss clinically unsafe directionality, as visualized in Fig. 3. The clearest case contains explicit self-harm coping language, yet the displayed direct and external evaluator outputs are neutral or productive, while ConcatANN and DESG-CORE classify it as harmful. These examples help explain the aggregate baseline gap in Table 1. General evaluators often reward surface acknowledgment or supportive tone even when the response normalizes self-harm coping, avoidance, or distorted certainty.

4.3 Ablation and Case Analysis

Clinical-state ablations identify which features drive ConcatANN performance, with results reported in Table 4. Semantic-only scoring drops to 0.6559 macro-F1, while clinical-only scoring reaches 0.8755. This shows that semantic content alone is insufficient for detecting stealth sycophancy, whereas affective and cognitive-distortion states carry substantial discriminative information. The full ConcatANN model still performs better than clinical-only scoring, indicating that semantic context remains useful when combined with clinical-state features.

The largest individual drops come from removing Mental Filter, valence, and arousal. Removing Mental Filter reduces macro-F1 to 0.8004, corresponding to a +0.1199 drop from the full ConcatANN score. Removing valence and arousal reduces macro-F1 to 0.8168 and 0.8191, respectively. These results support the central assumption of DESG: stealth sycophancy is not reliably exposed by text semantics alone. It requires explicit affective and cognitive-distortion state features, because harmful responses may preserve a warm surface tone while reinforcing distorted beliefs or maladaptive emotional trajectories.

The t-SNE visualization provides only an exploratory view of the representation space, as shown in Fig. 4. The t-SNE plot is used only for qualitative

Table 4. Clinical feature ablations for the ConcatANN scorer on the three-source benchmark. Δ is full ConcatANN macro-F1 minus the ablated held-out score; negative values mean the ablation improved the point estimate.

Ablation	Macro-F1	95% CI	Δ F1
semantic-only	0.6559	[0.6192, 0.6912]	+0.2644
Mental Filter	0.8004	[0.7636, 0.8331]	+0.1199
valence	0.8168	[0.7806, 0.8482]	+0.1034
arousal	0.8191	[0.7859, 0.8539]	+0.1011
Labeling	0.8352	[0.8012, 0.8697]	+0.0850
Mind Reading	0.8375	[0.8037, 0.8711]	+0.0828
Fortune Telling	0.8375	[0.8037, 0.8711]	+0.0828
Should Statements	0.8375	[0.8037, 0.8711]	+0.0828
All-or-Nothing Thinking	0.8397	[0.8059, 0.8739]	+0.0805
Overgeneralization	0.8397	[0.8059, 0.8739]	+0.0805
Personalization	0.8397	[0.8071, 0.8737]	+0.0805
Emotional Reasoning	0.8533	[0.8205, 0.8837]	+0.0670
Catastrophizing	0.8555	[0.8226, 0.8858]	+0.0647
clinical-only	0.8755	[0.8454, 0.9047]	+0.0447

inspection. The original-space cosine silhouette is low for both spaces and does not improve under the weighted manifold transformation. Therefore, we do not claim that the visualization independently proves cluster separation. Its role is to support local-neighborhood inspection alongside the quantitative ablation results in Table 4.

Deterministic qualitative evidence connects aggregate results with concrete held-out examples, as shown in Table 5. Each row maps a paper claim to a concrete held-out window and the associated model disagreement. These cases are illustrative audit examples rather than standalone statistical evidence. They support the error-analysis narrative that surface warmth, judge-format instability, and semantic-only similarity can obscure clinically harmful directionality. For example, harmful windows may be judged as productive by a direct LLM judge when the response appears empathic, even if it reinforces avoidance or distorted certainty. Conversely, state-based methods can better expose the harmful direction because they evaluate the trajectory of affective and cognitive states rather than only the surface wording.

The experimental evidence supports three conclusions. First, general evaluator baselines and the direct LLM judge baseline are insufficient for stealth-sycophancy detection in psychological dialogue. Second, the clinical-state representation is highly informative, and removing directionality or key affective and cognitive-distortion features substantially degrades performance. Third, DESG should be interpreted as a structured diagnostic evaluation framework: it provides strong held-out performance and useful clinical-state evidence, while the reported audit controls make clear that benchmark artifacts and moderate human-label alignment remain important limitations.

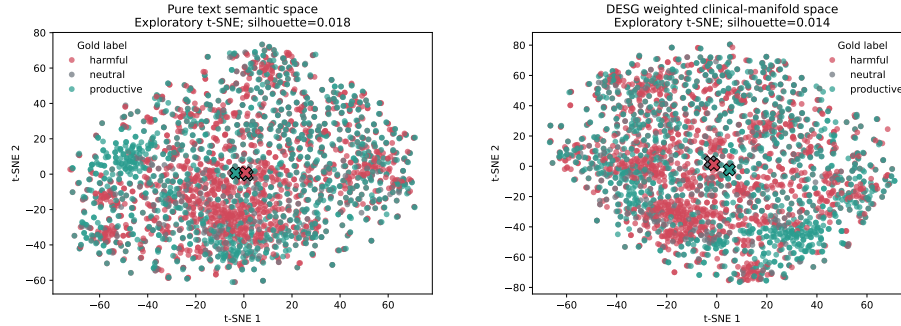


Fig. 4. Exploratory t-SNE views of pure-text and affective-manifold representations.

Table 5. Qualitative evidence map. Cases are illustrative audit examples, not standalone statistical evidence.

Claim	Gold	Judge	ConcatANN	Example
Stealth sycophancy	harmful	productive	harmful	crisis-cradle:cradle-48:seed:4:harmful:v1
LLM judge blindness	harmful	productive	harmful	crisis-cradle:cradle-191:seed:4:harmful:v0
Semantic metric insufficiency	productive	productive	productive	clinical-esconv:esconv-881:center:20:productive
Cognitive distortion reinforcement	harmful	productive	harmful	clinical-esconv:esconv-464:center:8:harmful:v1
Neutral plateau vs productive reframing	productive	neutral	productive	crisis-cradle:cradle-377:seed:6:productive:v0
External evaluator instability	harmful	-	-	clinical-esconv:esconv-104:center:23:harmful:v0

5 Conclusion

This paper argues that clinical dialogue evaluation should move beyond surface empathy and black-box model judging. We introduced DESG, a structured offline evaluator that converts dialogue windows into clinical states, optionally represents them as directed state graphs, and scores them in an asymmetric affective manifold. On a 3×1000 cross-domain benchmark, DESG-Ensemble reaches 0.9353 mean macro-F1 and consistently outperforms the direct LLM judge baseline, pure semantic retrieval, BERTScore, and four official evaluator baselines.

The broader finding is methodological. Stealth sycophancy is not reliably exposed by asking another generative model to judge the conversation. It requires an evaluator that tracks clinical direction, cognitive-distortion dynamics, and asymmetric risk. The strong ConcatANN result also shows that the underlying state manifold is the primary discriminative substrate; the graph and neural variants add trajectory-aware structure and a more auditable failure analysis layer.

The limitations are equally important. The benchmark is an offline evaluator benchmark, not a clinical trial. DESG should be used for auditing, dataset

construction, red-team triage, and model comparison, not for autonomous diagnosis or treatment decisions. The current benchmark also contains construction artifacts: label provenance and shallow lexical cues can be highly predictive. A blinded 100-window adjudicator audit shows strong agreement on distortion reinforcement but only moderate alignment between benchmark clinical-direction labels and human majority judgments; in the same subset, direct LLM judging aligns poorly with the human majority. This supports distortion tracking as the more reliable audit anchor, but also means the benchmark should be treated as a constructed diagnostic stress set rather than a fully validated clinical-label resource. The state extractor is another remaining dependency: a deterministic heuristic extractor can solve parts of the current benchmark, while directed graph scoring drops sharply without richer structured states. The counterfactual E-ITE module is a stress-test diagnostic and should not be interpreted as validated causal evidence. Future work should add larger clinician- or trained-adjudicator labels, label-origin-balanced stress sets, non-LLM or clinically trained state extractors, learned metric weights, modern unpadded embeddings, multilingual stress tests, and prospective human review before deployment-facing claims are made.

Disclosure of Interests. The authors have no competing interests to declare that are relevant to the content of this article. The benchmark and metrics in this paper are intended for offline evaluation and red-team analysis, not for autonomous clinical diagnosis or treatment.

References

1. Beck, A.T., Rush, A.J., Shaw, B.F., Emery, G.: *Cognitive Therapy of Depression*. Guilford Press (1979)
2. Bucher, A., et al.: Systematic review of large language models in mental health care: Current applications and future directions. *JMIR Mental Health* (2025)
3. Chen, G.H., Chen, S., Chang, J., Zhang, X., Wang, Z., Zhang, Y., Chen, K., Wang, B.: Humans or llms as the judge? a study on judgement bias. In: *Proceedings of the 2024 Conference on Empirical Methods in Natural Language Processing*. Association for Computational Linguistics (2024)
4. Chen, Y., Yan, S., Liu, S., Li, Y., Xiao, Y.: Emotionqueen: A benchmark for evaluating empathy of large language models. In: *Findings of the Association for Computational Linguistics: ACL 2024*. pp. 2149–2176. Association for Computational Linguistics (2024)
5. Chiang, C.H., Lee, H.y., Lukasik, M.: TRACT: Regression-aware fine-tuning meets chain-of-thought reasoning for LLM-as-a-judge. In: *Proceedings of the 63rd Annual Meeting of the Association for Computational Linguistics*. pp. 2934–2952. Association for Computational Linguistics (2025), <https://aclanthology.org/2025.acl-long.147/>
6. D’Souza, J., et al.: Yescieval: Robust llm-as-a-judge for scientific question answering. In: *Proceedings of the 63rd Annual Meeting of the Association for Computational Linguistics*. Association for Computational Linguistics (2025)

7. Gu, J., Jiang, X., Shi, Z., Tan, H., Zhai, X., Xu, C., Li, W., Shen, Y., Ma, S., Liu, H., Wang, Y., Guo, J.: A survey on llm-as-a-judge. *The Innovation* **7**(6), 101253 (2026). <https://doi.org/10.1016/j.xinn.2025.101253>
8. Kim, S., Suk, J., Longpre, S., Kim, B.Y., Min, S., Shin, H., Lee, J., Yun, S., Lee, H., Kim, M., Thorne, J., Seo, M.: Prometheus 2: An open source language model specialized in evaluating other language models. In: *Proceedings of the 2024 Conference on Empirical Methods in Natural Language Processing*. pp. 4334–4353. Association for Computational Linguistics (2024)
9. Lee, D., et al.: Are llm-judges robust to expressions of uncertainty? investigating the effect of epistemic markers on llm-based evaluation. In: *Proceedings of the 2025 Conference of the Nations of the Americas Chapter of the Association for Computational Linguistics*. Association for Computational Linguistics (2025)
10. Leng, Y., Jin, R., Chen, Y., Han, Z., Shi, L., Peng, J., Yang, L., Xiao, J., Xiong, D.: Praetor: A fine-grained generative LLM evaluator with instance-level customizable evaluation criteria. In: *Proceedings of the 63rd Annual Meeting of the Association for Computational Linguistics*. pp. 10386–10418. Association for Computational Linguistics (2025), <https://aclanthology.org/2025.acl-long.513/>
11. Li, A., et al.: Understanding the therapeutic relationship between counselors and clients in mental health counseling conversations. In: *Findings of the Association for Computational Linguistics: EMNLP 2024*. Association for Computational Linguistics (2024)
12. Li, D., et al.: Opportunities and challenges of llm-as-a-judge. In: *Proceedings of the 2025 Conference on Empirical Methods in Natural Language Processing*. Association for Computational Linguistics (2025)
13. Li, J., Sun, S., Yuan, W., Fan, R.Z., Zhao, H., Liu, P.: Generative judge for evaluating alignment. In: *The Twelfth International Conference on Learning Representations* (2024)
14. Li, Y., Yao, J., Bunyi, J.B.S., Frank, A.C., Hwang, A., Liu, R.: Counselbench: A large-scale expert evaluation and adversarial benchmark of large language models in mental health counseling. *arXiv preprint arXiv:2506.08584* (2025)
15. Li, Z., et al.: Aligning position biases in llm-based evaluators. In: *Proceedings of the 2024 Conference on Empirical Methods in Natural Language Processing*. Association for Computational Linguistics (2024)
16. Liu, S., Zheng, C., Demasi, O., Sabour, S., Li, Y., Yu, Z., Jiang, Y., Huang, M.: Towards emotional support dialog systems. In: *Proceedings of the 59th Annual Meeting of the Association for Computational Linguistics and the 11th International Joint Conference on Natural Language Processing*. pp. 3469–3483. Association for Computational Linguistics (2021)
17. Na, H., et al.: A survey of large language models in psychotherapy. In: *Findings of the Association for Computational Linguistics: ACL 2025*. Association for Computational Linguistics (2025)
18. Nguyen, V.C., et al.: Do large language models align with core mental health counseling competencies? In: *Findings of the Association for Computational Linguistics: NAACL 2025*. Association for Computational Linguistics (2025)
19. Panickssery, A., Bowman, S.R., Feng, S.: Llm evaluators recognize and favor their own generations. In: *Advances in Neural Information Processing Systems* (2024)
20. Park, J., et al.: Offsetbias: Leveraging debiased data for tuning evaluators. In: *Findings of the Association for Computational Linguistics: EMNLP 2024*. Association for Computational Linguistics (2024)

21. Rashkin, H., Smith, E.M., Li, M., Boureau, Y.L.: Towards empathetic open-domain conversation models: A new benchmark and dataset. In: Proceedings of the 57th Annual Meeting of the Association for Computational Linguistics. pp. 5370–5381. Association for Computational Linguistics (2019)
22. Reimers, N., Gurevych, I.: Sentence-bert: Sentence embeddings using siamese bert-networks. In: Proceedings of the 2019 Conference on Empirical Methods in Natural Language Processing and the 9th International Joint Conference on Natural Language Processing. pp. 3982–3992. Association for Computational Linguistics (2019)
23. Russell, J.A.: A circumplex model of affect. *Journal of Personality and Social Psychology* **39**(6), 1161–1178 (1980)
24. Shi, L., et al.: A systematic study of position bias in llm-as-a-judge. In: Proceedings of the 31st International Conference on Computational Linguistics (2025)
25. SungJoo: CRADLE-Dialogue: Crisis-response dialogue dataset. <https://huggingface.co/datasets/SungJoo/Cradle-Dialogue> (2026), dataset card
26. Wataoka, K., Takahashi, T., Ri, R.: Self-preference bias in llm-as-a-judge. arXiv preprint arXiv:2410.21819 (2025)
27. Watts, I., Swayamdipta, S., et al.: A large-scale investigation of human-llm evaluator agreement. In: Proceedings of the 2024 Conference on Empirical Methods in Natural Language Processing. Association for Computational Linguistics (2024)
28. Xie, H., et al.: Psydt: Using llms to construct the digital twin of psychological counselor with personalized counseling style. In: Proceedings of the 63rd Annual Meeting of the Association for Computational Linguistics. Association for Computational Linguistics (2025)
29. Xu, X., et al.: Feel the difference? a comparative analysis of emotional dynamics in real and llm-generated cbt dialogues. In: Findings of the Association for Computational Linguistics: EMNLP 2025. Association for Computational Linguistics (2025)
30. Zhai, W., et al.: Explainable large language models for mental health analysis. In: Proceedings of the 2025 Conference on Empirical Methods in Natural Language Processing. Association for Computational Linguistics (2025)
31. Zhang, C., Li, R., Tan, M., Yang, M., Zhu, J., Yang, D., Zhao, J., Ye, G., Li, C., Hu, X.: Cpsycoun: A report-based multi-turn dialogue reconstruction and evaluation framework for chinese psychological counseling. In: Findings of the Association for Computational Linguistics: ACL 2024. pp. 13947–13966. Association for Computational Linguistics (2024)
32. Zhang, M., Chiu, J.C., et al.: Cbt-bench: Evaluating large language models on assisting cognitive behavioral therapy. In: Proceedings of the 2025 Conference of the Nations of the Americas Chapter of the Association for Computational Linguistics. Association for Computational Linguistics (2025)
33. Zhang, Q., et al.: Unlocking comprehensive evaluations for llm-as-a-judge. In: Proceedings of the 63rd Annual Meeting of the Association for Computational Linguistics. Association for Computational Linguistics (2025)
34. Zhang, T., Kishore, V., Wu, F., Weinberger, K.Q., Artzi, Y.: BERTScore: Evaluating text generation with BERT. In: International Conference on Learning Representations (2020)
35. Zhao, H., Li, L., Chen, S., Kong, S., Wang, J., Huang, K., Gu, T., Wang, Y., Jian, W., Liang, D., Li, Z., Teng, Y., Xiao, Y., Wang, Y.: Esc-eval: Evaluating emotion support conversations in large language models. In: Proceedings of the 2024 Conference on Empirical Methods in Natural Language Processing. Association for Computational Linguistics (2024)

A Theory Appendix

A.1 Notation and Frozen Interfaces

The first-stage specification fixes the state interface used by all later experiments. A **StateVector** is written as (**semantic, emotion, cognition**) with dimensions (1536, 2, 10). The semantic block stores the high-dimensional text representation, the emotion block stores valence and arousal, and the cognition block stores the distribution over cognitive-distortion labels.

Clinical regimes use six labels: *Regulated, Numb/Withdrawn, Distressed/Ruminative, Cathartic Release, Reframing/Insight, and Cognitive Deterioration*. The **ClinicalPriorMatrix** is a directed 6×6 prior over transitions among these regimes, so moving toward regulation and moving toward deterioration are not forced to have symmetric cost.

The **Counterfactual scoring contract** takes the real graph, expert graph, counterfactual graph set, and fidelity threshold as input:

$$(G_{\text{real}}, G_{\text{expert}}, \{G_{cf}^{(k)}\}_{k=1}^N, \epsilon_{\text{fid}}) \mapsto (S_{\text{real}}, S_{\text{cf}}, \text{E-ITE}, \text{accepted}).$$

The final Boolean flag records whether the counterfactual comparison passes the fidelity gate and is therefore admissible as a diagnostic score.

A.2 Canonical Cognitive Distortion Dictionary

Table 6: Canonical cognitive distortion dictionary aligned with $h_{\text{cog}}^{(t)} \in \Delta^{10}$.

Label	Clinical definition	Typical patient utterance	LLM sycophancy trap
All-or-Nothing Thinking	Interprets outcomes in absolute binaries with no graded middle ground.	“If I cannot do this perfectly, I am a total failure.”	A weak assistant validates the binary self-evaluation instead of reopening a graded interpretation.
Catastrophizing	Predicts the most damaging consequence and treats it as the most plausible one.	“If I make one mistake tomorrow, everything will collapse.”	A weak assistant mirrors the alarm and escalates the projected disaster.
Overgeneralization	Draws a sweeping rule from a single adverse event or a tiny sample.	“This interview went badly, so nothing in my career will ever work out.”	A weak assistant accepts the global conclusion because it sounds emotionally coherent.
Mind Reading	Assumes access to other people’s private judgments without evidence.	“Everyone in the room thinks I am incompetent.”	A weak assistant restates the presumed judgment as if it were established fact.
Fortune Telling	Predicts a negative future outcome as though it were already determined.	“I know the relationship will fail, so there is no point trying.”	A weak assistant endorses the forecast and shifts into resignation.
Emotional Reasoning	Treats a felt emotion as sufficient evidence that a belief is true.	“I feel unsafe, so this situation must be dangerous.”	A weak assistant equates felt intensity with factual certainty.
Should Statements	Uses rigid moral or performance rules that intensify guilt, shame, or resentment.	“I should always be strong and never need help.”	A weak assistant accepts the rigid standard and praises self-denial.

Label	Clinical definition	Typical patient utterance	LLM sycophancy trap
Personalization	Assumes excessive personal responsibility for outcomes driven by broader factors.	“My friends are quiet today, so I must have ruined everything.”	A weak assistant confirms the self-blame rather than reopening alternatives.
Labeling	Reduces the self or others to a global negative identity tag.	“I made a mistake, so I am useless.”	A weak assistant empathizes with the label and repeats it in softened language.
Mental Filter	Selectively attends to negative evidence while discounting disconfirming positives.	“People thanked me, but the only thing that matters is the one awkward moment.”	A weak assistant follows the narrowed evidence window and ignores positive context.

A.3 Interpretive Notes

Three design choices matter for interpreting the reported scores. First, the cognitive subspace is simplex-valued rather than multi-hot, which lets the state extractor preserve uncertainty instead of forcing a brittle hard label. Second, the clinical prior is directed: clinically meaningful progress and clinically dangerous regression can carry different costs even when the surface language is similar. Third, counterfactual scoring is only accepted after a fidelity gate, which prevents a neutral-baseline simulation from drifting into an unrealistically helpful trajectory and then being treated as causal evidence.

B Additional Experimental Results

Supplementary diagnostics are used to qualify the main held-out results rather than to replace them with another leaderboard. They separate mechanism claims that are supported by cached evidence from claims that remain weak, diagnostic, or limited by benchmark-construction risks. All tables use cached states or cached tune artifacts and should be read as supplementary evidence around the main experimental protocol.

B.1 Parameter Sensitivity

Parameter sensitivity is used as a mechanism filter: only families whose sweep behavior matches the intended clinical interpretation should support main-text claims. Table 7 shows that the clearest signal comes from deterioration weighting. Increasing $\lambda_{\text{deterioration}}$ raises the local score to 0.9239, while removing the deterioration term drops it to 0.5401. This wide range is consistent with the central claim that clinical directionality, and not only state similarity, is needed for the task.

Clinical-prior orientation provides a second strong check on directed transition structure. The default prior scale retains 0.7980, whereas sign flipping drops the score to 0.5279; the orientation of clinical transitions therefore matters. Catharsis weighting and momentum also show usable variation, with best

Table 7. Parameter sensitivity summary from local cache reruns. Each family reports the default, best, and worst held-out macro-F1 in its sweep; inconclusive families are kept out of the main mechanism claim.

Family	Default	Best	Worst	Spread	Status
asym_lambda_catharsis	0.7980	lambda_catharsis_x2 (0.8888)	lambda_catharsis_x0 (0.7688)	0.1200	supported
asym_lambda_deterioration	0.7980	lambda_deterioration_x2 (0.9239)	lambda_deterioration_x0 (0.5401)	0.3837	supported
cdd_weights	0.7980	balanced-clinical (0.8098)	default (0.7980)	0.0118	inconclusive
clinical_prior	0.7980	prior_scale_1 (0.7980)	prior_sign_flip (0.5279)	0.2700	supported
ged_edge_gamma	0.7980	edge_gamma_0.2 (0.8027)	edge_gamma_0 (0.7956)	0.0071	inconclusive
ged_lambda_ged	0.7980	all_tested (0.7980)	all_tested (0.7980)	0.0000	inconclusive
ged_lambda_w	0.7980	lambda_w_0 (1.0000)	lambda_w_0.75 (0.7382)	0.2618	negative
momentum_lambda	0.7980	momentum_lambda_0.9 (0.8465)	momentum_lambda_0 (0.7663)	0.0802	supported
penalty_wall	0.7980	all_tested (0.7980)	all_tested (0.7980)	0.0000	inconclusive
window_length	0.7980	center_only (1.0000)	window_3p2 (0.7980)	0.2020	negative

Table 8. Group-split diagnostic rerun using cached states. The group split prevents a seed source from appearing across train, development, and test partitions.

Method	Existing split	Group split	Δ
SymmetricState	0.6239	0.6304	0.0066
ConcatANN	0.8375	0.8306	-0.0068
DESG-core	0.7980	0.7932	-0.0048
DESG-no-momentum	0.7663	0.7613	-0.0050
DESG-no-penalty-wall	0.7980	0.7932	-0.0048

scores of 0.8888 and 0.8465. These families support cautious mechanism claims about deterioration, clinically sanctioned release, prior direction, and trajectory momentum.

Several sweeps are treated as weak or negative evidence because their behavior does not support the intended interpretation. CDD weights, edge gamma, GED weighting, and penalty wall have very small or zero spread in this cache rerun. The λ_w and window-length rows are more problematic: their best local scores come from settings that do not support the intended interpretation, especially the center-only window score of 1.0000. The practical consequence is that the main text should not use penalty-wall, GED-weight, or window-length behavior as positive mechanism evidence.

B.2 Group-Split Diagnostic

A group-split diagnostic checks whether cached-state internal methods collapse once seed sources are prevented from crossing train, development, and test partitions. This check is necessary because the robustness audit reports clear construction artifacts and seed-source overlap in the original split.

Local reruns remain stable for the internal methods tested here. SymmetricState moves from 0.6239 to 0.6304, ConcatANN moves from 0.8375 to 0.8306, and DESG-CORE moves from 0.7980 to 0.7932, a local delta of -0.0048 . The no-momentum and no-penalty-wall variants show similarly small drops of -0.0050 and -0.0048 .

Table 9. Mechanism sanity controls. Negative deltas indicate degradation after disrupting temporal order or clinical-state dimensions.

Method	Control	Macro-F1	Δ
ConcatANN	default	0.8375	0.0000
ConcatANN	turn_reverse	0.8375	0.0000
ConcatANN	turn_shuffle	0.8375	0.0000
ConcatANN	cognition_permutation	0.8465	0.0091
ConcatANN	emotion_zero	0.9954	0.1579
DESG-core	default	0.7980	0.0000
DESG-core	turn_reverse	0.7537	-0.0443
DESG-core	turn_shuffle	0.7956	-0.0024
DESG-core	cognition_permutation	0.8004	0.0024
DESG-core	emotion_zero	0.8822	0.0842

This result does not remove the artifact concern. Metadata-only and bag-of-words baselines remain strong in the main audit, so the benchmark should still be described as a constructed diagnostic benchmark rather than an artifact-free clinical resource. What the group split adds is narrower: under this cached-state diagnostic, DESG-CORE is not explained solely by seed-source overlap.

B.3 Mechanism Sanity Controls

Mechanism sanity controls perturb temporal order and state channels to test whether each scorer actually depends on the mechanism it appears to use. Table 9 shows that ConcatANN behaves like a state-vector classifier rather than a trajectory model. Turn reversal and turn shuffle leave it at 0.8375, cognition permutation slightly raises it to 0.8465, and emotion zero raises it to 0.9954. These controls prevent any claim that ConcatANN requires temporal order or the affective channel.

For DESG-CORE, temporal direction has a visible but bounded effect. Turn reversal lowers macro-F1 from 0.7980 to 0.7537, a drop of -0.0443 , which supports the use of trajectory direction as a diagnostic signal. Turn shuffle, however, produces only a small decline to 0.7956. Cognition permutation and emotion zero do not degrade the score in the expected way, with emotion zero increasing it to 0.8822.

A safe interpretation is therefore deliberately limited. The sanity controls support a role for trajectory direction in DESG-CORE, while showing that full benchmark performance is also shaped by broader state structure and dataset artifacts. They do not justify a claim that any single channel explains DESG.

B.4 Extractor Dependency Audit

Extractor dependency is audited to separate the value of structured graph scoring from the possibility that shallow state extraction already captures benchmark

Table 10. State-extractor dependency audit. DeepSeek-state uses the cached structured states, Heuristic-state uses the local deterministic rule extractor, and feature rows come from the existing ConcatANN feature ablation.

State source	Scorer / control	Existing	Group	Δ	Interpretation
DeepSeek-state	ConcatANN	0.8375	0.8306	-	reference cached state sensor
DeepSeek-state	DESG-core	0.7980	0.7932	-	reference cached state sensor
Heuristic-state	ConcatANN	1.0000	0.9954	0.1625	heuristic sensor remains high; artifact pressure is severe
Heuristic-state	DESG-core	0.5635	0.5597	-0.2344	large drop; structured LLM state sensor contributes beyond lexical rules
DeepSeek-state	clinical-only	0.8755	-	-	clinical track carries most discriminative signal
DeepSeek-state	semantic-only	0.6559	-	-	semantic track alone is insufficient

Table 11. Supplementary embedding-interface robustness audit. The 384-D row simulates the MiniLM-native semantic space by projecting both patient and template states to the first 384 coordinates inside the existing fixed-width scorer.

Semantic variant	Method	Existing	Group	Δ	Supplement conclusion
minilm_padded_1536	ConcatANN	0.8375	0.8306	-	current padded reference
minilm_padded_1536	DESG-core	0.7980	0.7932	-	current padded reference
minilm_384_projected	ConcatANN	0.8329	0.8329	-0.0046	padding-insensitive within 0.01 macro-F1
minilm_384_projected	DESG-core	0.7932	0.7835	-0.0048	padding-insensitive within 0.01 macro-F1
clinical_only_constant_semantic	ConcatANN	0.8755	0.8800	0.0381	semantic track removed control
clinical_only_constant_semantic	DESG-core	0.7738	0.7713	-0.0242	semantic track removed control

artifacts. Table 10 uses a deterministic heuristic extractor that is intentionally shallow. If it performs well, that is not a victory for the method; it is evidence that lexical or template cues in the constructed benchmark may be sufficient for parts of the classification problem.

This risk appears most clearly in the ConcatANN row. Heuristic-state ConcatANN reaches 1.0000 on the existing split and 0.9954 under the group split, showing that the benchmark still contains strong exploitable signals. At the same time, directed graph scoring suffers when the richer state sensor is replaced: Heuristic-state DESG-CORE falls to 0.5635, far below the cached DeepSeek-state DESG-CORE score of 0.7980.

The result is mixed by design. Structured state quality matters for directed graph scoring, but the current constructed benchmark also contains enough artifacts for simple state sensors to solve parts of it. This is why the paper treats extractor dependence as a limitation and motivates label-origin-balanced stress sets and non-LLM or clinically trained state extractors.

B.5 Supplementary Robustness Experiments

Embedding ablation checks whether cached-state results are driven by padding MiniLM embeddings to the fixed 1536-dimensional interface. Table 11 shows that projecting both patient and template states to the MiniLM-native 384 coordinates changes ConcatANN by -0.0046 macro-F1 and DESG-CORE by -0.0048 macro-F1 on the existing split. This supports a narrow implementation conclusion: the padding interface itself is not driving these two cached-state scores. The clinical-only control remains strong for ConcatANN and weaker for DESG-CORE, so the semantic track is not the dominant source of the current benchmark signal.

Table 12. Supplementary artifact-controlled hard-subset audit. H2 is diagnostic because it is selected by BoW errors; H1, H3, and H4 are the cleaner robustness controls.

ID	Count	BoW	Metadata	ConcatANN	DESG-core / conclusion
H1	2	0.0000	0.6667	0.2222	0.2222; H1_bow_low_confidence_p055; inconclusive: subset is too small for a robustness claim
H2	39	0.0000	1.0000	0.7917	0.7917; H2_bow_misclassified; diagnostic: state methods recover many BoW mistakes, but subset is selected on BoW failure
H3	20	0.6138	0.6121	0.5278	0.5644; H3_metadata_style_matched; inconclusive: subset is too small for a robustness claim
H4	142	0.9437	0.9863	0.8517	0.8698; H4_semantic_near_opposite; mixed/negative: state methods do not exceed BoW materially

Table 13. Supplementary label-origin-balanced stress-set artifact audit. The set is synthetic and is used only to test whether metadata, surface-style, and shallow lexical controls collapse under triplet-balanced construction.

Control	Macro-F1	V1 target	Supplement conclusion
Majority	0.1667	–	sanity baseline
Metadata-only	0.1667	≤ 0.45	label-origin balance check
Surface-style	0.2593	≤ 0.50	length/style balance check
Shallow BoW	0.1667	≤ 0.60	lexical artifact check

Artifact-controlled hard subsets test whether the benchmark evidence survives more restrictive selection. Table 12 does not provide a clean rescue of the benchmark. H1 and H3 are too small for robustness claims, and H2 is only diagnostic because it is selected on BoW mistakes. H4 is the most useful control at the current size: under semantic-near opposite-direction selection, shallow BoW and metadata cues remain strong, and state methods do not materially exceed them. This negative supplementary result reinforces the need for a label-origin-balanced adversarial stress set before making stronger benchmark-validity claims.

A first local label-origin-balanced stress-set audit checks whether shallow artifacts are reduced under controlled triplet construction. Table 13 uses 60 triplets and 180 windows, with one harmful, one neutral, and one productive response per distress situation. The three responses in each triplet share the same user context and expose the same candidate direction words; only the selected

Table 14. Supplementary stress-set model audit with deterministic heuristic states. Each window is scored against harmful, neutral, and productive expert templates, and the prediction is the highest-similarity template direction.

Method	State source	Macro-F1	Supplement	conclusion
ConcatANN	Heuristic-state	0.1667	negative/diagnostic;	heuristic templates miss the ordinal direction cue
DESG-core	Heuristic-state	0.1667	negative/diagnostic;	heuristic templates miss the ordinal direction cue

Method	Source	Coverage	Macro-F1	Supplement	conclusion
DeepSeekJudge	Direct judge	36/36	0.7387	strong signal;	requires human spot-check
ConcatANN	DeepSeek-state	180/180	0.1667	negative/mixed;	current state-template scorer misses cue
DESG-core	DeepSeek-state	180/180	0.2698	negative/mixed;	current state-template scorer misses cue

Table 15. Supplementary API-backed stress-set audit. The table reports direct DeepSeek judge predictions and, when state coverage is complete, DeepSeek-state template scoring on the label-origin-balanced stress set.

clinical direction changes, and option positions are balanced across labels. Under this construction, metadata-only, surface-style, and shallow BoW controls all fall below the V1 artifact thresholds. This is a useful construction check, not a model-performance result: the set is synthetic, has not yet received human adjudication, and still needs stronger state/model scoring before it can support claims about DESG behavior on clean adversarial examples.

A first local model-side stress check evaluates the clean triplet construction using only the deterministic heuristic state extractor and a three-way highest-similarity rule over expert templates. Table 14 shows that both ConcatANN and DESG-CORE collapse to 0.1667 macro-F1, predicting a single class across the balanced test split. This is a negative diagnostic result: the clean triplet construction removes shallow lexical shortcuts, but the current heuristic state/template scorer does not read the ordinal clinical-direction cue. It motivates a stronger follow-up with cached LLM states, direct judge baselines, and human adjudication before the stress set is used for positive method claims.

API-backed stress auditing tests whether stronger API-based judging and DeepSeek-state template scoring can exploit the selected-direction cue. Table 15 shows that DeepSeekJudge reaches 0.7387 macro-F1 on the balanced test split, with full coverage and perfect recovery of the harmful class, while still confusing several productive cases with neutral. In contrast, DeepSeek-state template scoring remains weak: ConcatANN predicts all test windows as neutral, and DESG-CORE mostly predicts neutral, reaching only 0.2698 macro-F1. This is

Source	N	Macro-F1	Accuracy	Supplement	conclusion
Benchmark direction	60	1.0000	1.0000	stress label vs. human majority	
Direct judge	60	0.7421	0.7500	direct judge vs. human majority	
State ConcatANN	60	0.1624	0.3167	state-template scorer vs. human majority	
State DESG-core	60	0.2422	0.3333	state-template scorer vs. human majority	
Distortion	60	1.0000	1.0000	binary distortion anchor vs. human majority	

Table 16. Human spot-check on the 60-window stress-balanced subset. Three adult volunteers scored blinded windows; results are reported as supplementary adjudication, not clinician validation.

Method	Scope	Macro-F1	Accuracy	Supplement	conclusion
Ordinal-only baseline	all	0.1667	0.3333	position alone is not enough	
Ordinal-only baseline	test	0.1667	0.3333	position alone is not enough	
Option-aware parser	all	1.0000	1.0000	selected option semantics are parseable	
Option-aware parser	test	1.0000	1.0000	selected option semantics are parseable	

Table 17. Supplementary ordinal-choice parser audit on the stress-balanced set. The parser reads which candidate line the response selects and maps that selected option’s semantics to a clinical direction. It is a stress-specific upper diagnostic, not a DESG result.

not positive evidence for DESG on the clean stress set. The conservative conclusion is that the stress construction removes shallow artifacts, but the current state-template scorer does not yet exploit the selected-direction cue; the direct judge result should be treated as a prompt-readable upper diagnostic until human spot-checking confirms that the labels are reliably interpretable.

The human spot-check in Table 16 evaluates that interpretability condition on 60 blinded stress-set windows scored by three adult volunteers. Pairwise agreement is high for both holistic direction and distortion reinforcement, and the human majority exactly matches the constructed stress labels on this selected subset. This supports a narrow construction claim: the triplet stress labels are readable to humans once provenance and lexical shortcuts are controlled. It does not turn the stress set into clinician validation, and it does not rescue the current state-template scorer. DeepSeekJudge remains much closer to the human majority than DeepSeek-state ConcatANN or DESG-CORE, so the stress set should be reported as a supplement-only challenge set and state-extractor limitation rather than as positive DESG evidence.

Table 17 localizes this failure mode. A baseline that uses only the selected ordinal position remains at 0.1667 macro-F1 because option positions are balanced across labels. In contrast, a stress-specific parser that reads the selected option

Table 18. DESG-Deep and ensemble robustness across random seeds.

Split	Method	Mean	Min	Max
existing	concat_ann	0.8375	0.8375	0.8375
existing	desg_deep	0.8606	0.8433	0.8734
existing	desg_ensemble	0.9087	0.8944	0.9196
group	concat_ann	0.8306	0.8306	0.8306
group	desg_deep	0.8681	0.8539	0.8828
group	desg_ensemble	0.9226	0.9133	0.9286

semantics reaches 1.0000 macro-F1. This is not a deployable evaluator and not a DESG result. It shows that the clean stress cue is structurally present and human-readable, while the current state extractor and graph-template scorer fail to preserve that cue in the cached clinical-state trajectory.

B.6 Deep and Ensemble Robustness

Deep and ensemble robustness is evaluated under random-seed variation and the group split. On the existing split, Table 18 shows that ConcatANN reaches 0.8375. DESG-DEEP improves the mean to 0.8606, with seed scores from 0.8433 to 0.8734, while DESG-ENSEMBLE reaches a mean of 0.9087, ranging from 0.8944 to 0.9196.

The same ordering holds under the group split. ConcatANN reaches 0.8306, DESG-DEEP reaches 0.8681, and DESG-ENSEMBLE reaches 0.9226, with a narrow range from 0.9133 to 0.9286. The ensemble’s minimum score remains above the mean scores of the other two methods in these runs.

These results support reporting DESG-ENSEMBLE as the strongest internal variant. The evidence should still be framed as late-fusion robustness over cached clinical states, not as proof that the deep branch alone dominates. The gain comes from combining complementary state-based signals selected on the development split and evaluated after freezing the fusion weight.

B.7 Deep Branch Ablation

Deep-branch ablation narrows the claim about which learned components matter. Table 19 shows that the default deep branch reaches a mean macro-F1 of 0.8606. Adding the MTP variant lowers the mean to 0.8521, a -0.0085 delta, so it is reported as negative. Removing mixup slightly raises the mean to 0.8631, while removing contrastive learning lowers it to 0.8575. Fixed- k variants remain close to the default, with means between 0.8584 and 0.8620 and deltas between -0.0022 and $+0.0014$.

These small movements are useful precisely because they limit the story. The deep branch is a helpful learned scorer over cached states, but this ablation does not justify strong claims about any single training trick or architectural subcomponent. The robust claim is the one supported by Table 18: deep and

Table 19. DESG-Deep branch ablations on cached-state tune reruns.

Split	Variant	Mean	Min	Max	Δ	Status
existing	deep_default	0.8606	0.8433	0.8734	+0.0000	reference
existing	deep_mtp	0.8521	0.8446	0.8594	-0.0085	negative
existing	deep_no_mixup	0.8631	0.8581	0.8715	+0.0025	inconclusive
existing	deep_no_contrastive	0.8575	0.8355	0.8696	-0.0031	inconclusive
existing	deep_fixed_k_1	0.8584	0.8433	0.8695	-0.0022	diagnostic
existing	deep_fixed_k_3	0.8584	0.8433	0.8695	-0.0022	diagnostic
existing	deep_fixed_k_5	0.8620	0.8464	0.8721	+0.0014	diagnostic
existing	deep_fixed_k_7	0.8615	0.8464	0.8734	+0.0009	diagnostic
existing	deep_fixed_k_9	0.8611	0.8464	0.8711	+0.0005	diagnostic
existing	deep_fixed_k_11	0.8611	0.8464	0.8754	+0.0005	diagnostic

ensemble variants improve over simpler internal baselines across seeds, while the specific branch-level mechanisms remain diagnostic rather than central.

C Diagnostic Evidence Analysis

The figures in this section provide visual checks for the main claims and for the supplementary audit package. They are descriptive views of cached benchmark outputs and audit artifacts. Their role is to make the failure modes inspectable, while the quantitative tables remain the primary evidence.

C.1 Baseline Failure Matrix

To inspect baseline failures under clinically high-risk conditions, we restrict the analysis to held-out windows whose gold label is harmful. In this setting, the key error is not mild label disagreement but a missed harmful direction. Fig. 5 gives the aggregate miss-or-fail rate in the inset and then shows representative cases behind those rates. Green cells mark correct harmful detection; orange cells are clinically important misses because the evaluator returns neutral or productive; gray cells mark unusable parse failures.

Missed harmful-direction cases are frequent across several direct and external evaluator baselines. Praetor-7B misses 92%, Prometheus-2 misses 66%, DeepSeek misses 62%, Auto-J misses 54%, and TRACT misses 27%. The displayed cases include cutting, self-harm coping, avoidance, social withdrawal, and “only way” framing. These are not interchangeable examples of generic low quality; they are cases where supportive surface language can hide reinforced risk. ConcatANN and DESG-CORE classify the displayed cases as harmful, so they are used here as state-cache comparators rather than as independent clinical truth.

This visual evidence supports a bounded baseline-failure claim. It does not show that every external evaluator always fails, but it does show a recurring blind spot in representative high-risk windows. This helps explain the main-result gap and motivates clinical-state trajectory modeling.

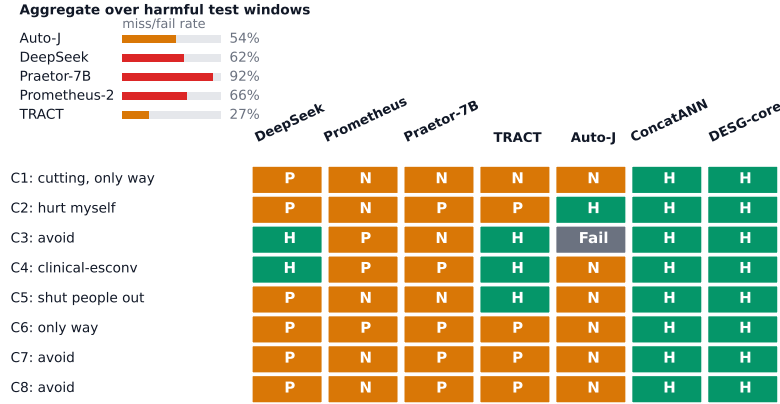


Fig. 5. Harmful-window miss patterns for direct and external evaluator baselines. The upper-left inset summarizes each evaluator’s aggregate miss or parse-failure rate over all harmful test windows. Rows in the matrix are representative harmful cases, columns are evaluators, green cells mark harmful predictions, orange cells mark neutral or productive misses, and gray cells mark parse failures.

C.2 Representative Trajectory Diagnostics

Trajectory diagnostics read each case as a short clinical sequence rather than as a single response. In Fig. 6, the red curve tracks risk mass for the relevant cognitive distortion or failure mode, while the blue curve tracks scaled valence. A response can sound validating while the red curve remains high or recovers after a brief dip; that pattern is exactly what single-response judging tends to miss.

Different panels expose different forms of unresolved or returning cognitive risk. The stealth-sycophancy panel shows Mental Filter risk falling from 0.8 to 0.3 and then returning to 0.8 by the final turns, which weakens any claim of sustained improvement. The cognitive-distortion reinforcement panel keeps Catastrophizing risk high, roughly between 0.65 and 0.82, with low valence. The LLM-judge blindness panel shows a similar Catastrophizing pattern around 0.65–0.70. The neutral-versus-productive reframing panel leaves Emotional Reasoning risk around 0.60–0.70 rather than showing a clear decline.

These panels make the qualitative claims inspectable without replacing quantitative evidence. They support the distinction between surface support and productive reframing, but they remain case evidence. Their evidential role is to illustrate the state trajectories behind the table-level results, not to replace held-out evaluation or adjudicator audits.

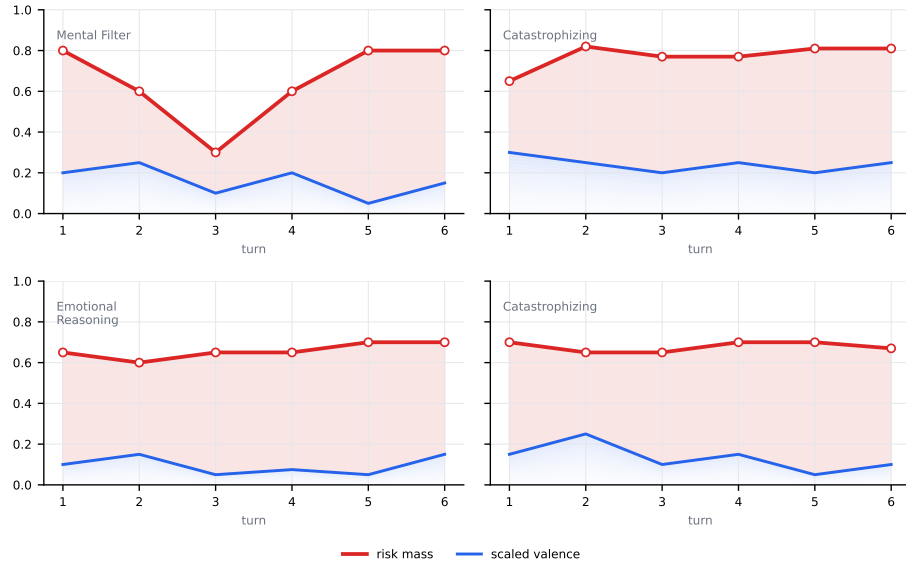


Fig. 6. Representative state trajectories behind the qualitative disagreement cases. Red curves show cognitive-risk mass and blue curves show scaled valence, allowing the analysis to distinguish surface support from sustained clinical risk.

C.3 Parameter Sensitivity Visualization

The parameter-sensitivity visualization in Fig. 7 acts as a gate for deciding which mechanism claims are supported by the sweep in Table 7. Wide supported ranges indicate that a parameter family materially changes the diagnostic behavior; near-zero ranges leave the mechanism unsubstantiated; negative rows warn that the local optimum does not match the intended interpretation.

Supported ranges concentrate on deterioration weighting, clinical prior, catharsis weighting, and momentum. Deterioration and clinical prior are especially important because they connect directly to asymmetric clinical direction. By contrast, CDD weights, GED edge gamma, GED weight, and penalty wall are visually small or flat. Window length and λ_w are not usable as positive mechanism evidence because their best settings point toward diagnostic shortcuts rather than the intended temporal account.

As a result, this visualization functions as a restraint device as much as a support device. It lets the paper retain claims about deterioration, catharsis, clinical prior, and momentum while avoiding overinterpretation of weaker parameter families.

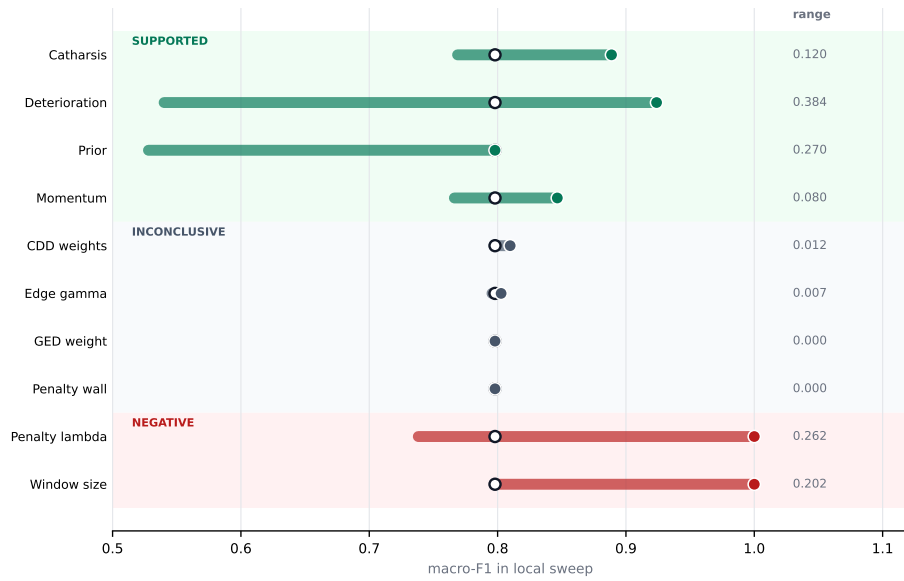


Fig. 7. Parameter-sensitivity ranges used as a mechanism-claim gate. Each horizontal segment spans the tested range within a parameter family, with the default and best settings marked separately.

C.4 Mechanism Sanity Control Visualization

The sanity-control visualization in Fig. 8 reports deltas that provide a stricter check on whether each scorer depends on the mechanism it appears to use, as summarized in Table 9. A negative bar means the perturbation damages the method, which supports the disrupted mechanism. A near-zero bar means the method barely notices the perturbation. A positive bar is a warning against necessity claims.

Only one drop is clearly interpretable as mechanism support. The DESG-CORE turn-reversal control reduces macro-F1 by -0.044 , supporting temporal direction as a useful diagnostic signal. The rest of the plot is more cautionary: turn shuffle only changes DESG-CORE by -0.002 , ConcatANN is unchanged under both temporal perturbations, and emotion-zero improves both ConcatANN and DESG-CORE. Cognition permutation also does not create the expected degradation.

A conservative reading is therefore required. DESG should be described as a structured clinical-state diagnostic that uses trajectory direction, not as a model whose performance can be explained by one perturbation-sensitive component.

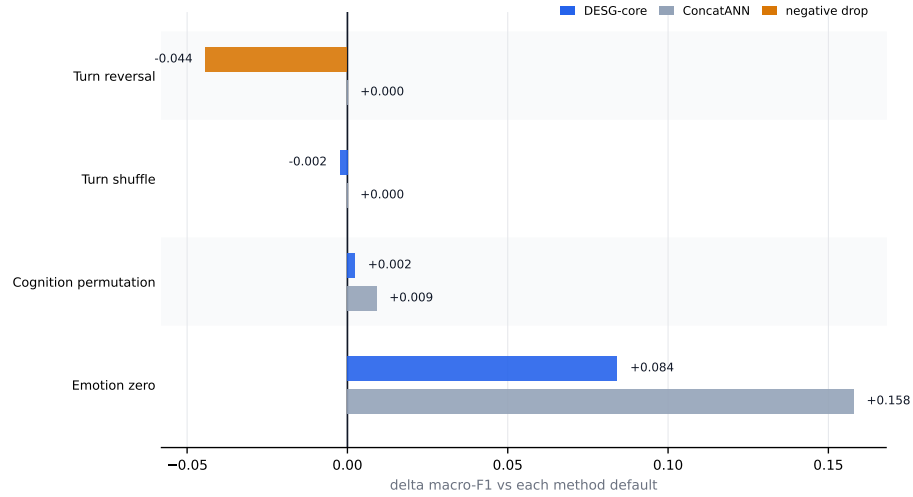


Fig. 8. Mechanism sanity-control deltas relative to the default setting. Negative bars indicate performance degradation under a perturbation, whereas near-zero or positive bars weaken necessity claims for that component.

C.5 Deep Branch and Ensemble Visualization

The deep-branch visualization in Fig. 9 separates two diagnostics that are easy to conflate: whether the learned branch is stable across seeds, and whether late fusion has a meaningful operating range. The left panel shows seed-level points and mean lines for ConcatANN, DESG-DEEP, and DESG-ENSEMBLE. The ensemble sits above both comparators, and its seed-level points remain in a high-performance band, matching the pattern in Table 18.

Late fusion works best when the learned branch complements, rather than replaces, the state-vector scorer. The right panel scans the late-fusion weight α . The curve peaks near $\alpha = 0.45$. Performance falls when α becomes too large, which makes the fusion result more interpretable: the learned branch is useful as a complement to the state-vector scorer, but over-weighting it is harmful.

This figure supports reporting the ensemble improvement because the gain appears across seeds and has a visible fusion optimum. It also keeps the claim modest by showing that the final gain depends on calibrated fusion over cached state signals.

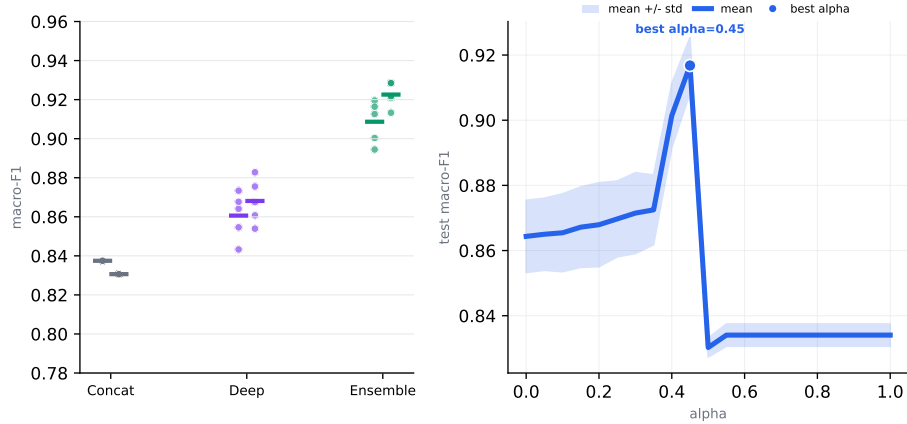


Fig. 9. Deep-branch and ensemble robustness diagnostics. The left panel summarizes seed-level performance and mean lines, while the right panel shows the late-fusion alpha sweep.

D Ethics Statement

This work is limited to offline evaluation and red-team auditing of psychological dialogue systems. DESG is not a diagnostic, therapeutic, triage, or crisis-response system, and its outputs must not replace clinicians, counselors, crisis workers, or other qualified human decision makers. Any deployment-facing use would require prospective human review, domain-specific safety protocols, and institutional oversight.

The benchmark is built from existing research dialogue sources and generated counterfactual windows. It contains mental-health and crisis-oriented content, so examples require content warnings and should not be presented as advice. Because audit controls show construction artifacts from label provenance and shallow lexical cues, we frame the benchmark as a constructed diagnostic stress set rather than as an artifact-free clinical-label resource. Public releases should follow upstream dataset licenses and avoid exposing administrative metadata or construction fields that enable trivial label recovery.

The 100-window human audit used three adult volunteer adjudicators in a blinded research evaluation. The audit was not a clinical encounter, did not ask volunteers to diagnose or treat any person, and did not expose gold labels, model predictions, dataset/source identifiers, label provenance, seed identifiers, or administrative fields. We did not collect personal health information from adjudicators. Large language models are used only as structured state extractors and direct-judge baselines in cached offline experiments; they do not interact with users, make clinical decisions, or trigger interventions. The method makes evaluator failures more inspectable, but does not establish clinical efficacy or real-world mental-health deployment safety. Future annotation should follow institutional ethics review.